

Focusing, Power Tunneling and Rejection from Chiral and/or Chiral Nihility/Nihility Metamaterials Layers

By

Syed Touseef Hussain Shah¹, Faiz Ahmad², Aqeel A. Syed³, Qaisar Abbas Naqvi⁴

¹touseefshah1 @ yahoo.com, ²faizsolangi @ gmail.com,

³aqeel @ qau.edu.pk, ⁴qaisar @ qau.edu.pk

^{1,3,4} Department of Electronics, Quaid-i-Azam University, 45320, Islamabad

² Department of Electronics, CIIT, Islamabad

ABSTRACT

Focusing of electromagnetic plane wave from a large size paraboloidal reflector, composed of layers of chiral and/or chiral nihility metamaterials, has been studied using Maslov's method. First, the transmission and reflection of electromagnetic plane wave from two parallel layers of chiral and/or chiral nihility metamaterials are calculated using transfer matrix method. The effects of change of angle of incidence, chirality parameters and impedances of layers are noted and discussed. Special cases by taking very large and small values of permittivity of second layer, while assuming value of corresponding chirality equal to zero, are also treated. These special cases are equivalent to reflection from a perfect electric conductor backed chiral layer and nihility backed chiral layer, respectively. Results of reflection from parallel layers have been utilized to study focusing from a large size paraboloidal reflector. The present study, on focusing from a paraboloidal reflector, not only unifies several published works conducted by different researchers but also provides better understanding of new cases.

1.0 Introduction

Chiral media, have been well known for a long time due to some interesting properties, exhibiting in the optical range of frequencies. Out of these properties, optical activity and circular dichroism are of practical interest [1-6]. Chiral medium can be thought as composed of numerous randomly oriented chiral objects which can never be brought into congruence with their mirror images by any translation or rotation [7-10]. Many chiral objects are found in nature such as irregular tetrahedrons, sugar molecules and wire helices. In fact the word “chirality” is derived from the greek word “cheir” having meaning of hand; an object possessing above mentioned property. In science particular word “chirality” instead of dissymmetry was first introduced by Lord Kelvin, Professor of natural philosophy in the University of Glasgow. Now this word is used to describe the media microscopically composed of the chiral objects.

When linearly polarized wave falls on a slab of chiral medium, it splits into two circularly polarized waves: one left circularly polarized and the other right circularly polarized [8-10]. After passing through the slab the two waves combine to yield a linearly polarized wave whose plane of polarization is rotated with respect to the plane of polarization of the incident wave. Effect of chirality of the medium which rotates the plane of linearly polarized wave passing through it is studied by Biot, Arago and Friesnel. This phenomenon is named as optical activity. The amount of rotation depends upon the distance traveled by the wave in the slab. This phenomenon is named as circular birefringence. Circular dichroism represents the phenomenon of different amount of field absorption for the left and right circularly polarized waves as they pass through the chiral media. The constitutive relations for chiral metamaterial [8] are

given below,

$$\mathbf{D} = \epsilon\mathbf{E} + i\kappa\mathbf{H} \quad (1)$$

$$\mathbf{B} = \mu\mathbf{H} - i\kappa\mathbf{E} \quad (2)$$

The behavior of propagation and radiation of the field in a chiral medium has been investigated by several authors [8-10].

Left-handed materials are those materials in which electric, magnetic and the wave vector follow the left hand rule. Veselago introduced the concept of negative refraction for the materials obeying left hand rule [11]. In chiral medium, negative real parts of the permittivity and permeability lead an isotropic chiral medium to exhibit circular dichroism that is reverse with respect to that exhibited by an identical medium but with positive real parts of permittivity and permeability. These left handed materials exhibit some interesting properties such as backward wave and double negative parameters [12]. Negative refraction can also be achieved by using the chiral metamaterials [13-16]. In chiral metamaterials strong enough chirality produces negative refractive index for one of the eigenwaves [17-18].

In electromagnetics, Lakhtakia introduced the concept of nihility metamaterial for such a material whose permittivity and permeability approaches to zero [19]. Constitutive relations for nihility metamaterial are,

$$\mathbf{D} = 0 \quad (3)$$

$$\mathbf{B} = 0 \quad (4)$$

Lakhtakia showed that propagation is not possible in nihility metamaterial. Later, Tretyakov et al. [20] extended this concept of nihility for the isotropic chiral medium.

A special case of chiral metamaterial is called chiral nihility metamaterial for which at certain value of frequency, real parts of permittivity and permeability both are simultaneously zero. That is, $\epsilon \rightarrow 0$, $\mu \rightarrow 0$ and $\kappa \neq 0$ at nihility frequency. Constitutive relations for chiral nihility metamaterials become as,

$$\mathbf{D} = i\kappa\mathbf{H} \quad (5)$$

$$\mathbf{B} = -i\kappa\mathbf{E} \quad (6)$$

Chiral nihility metamaterial has two wavenumbers of equal magnitude and opposite signs. When a dielectric-chiral nihility half space is excited by an oblique incident linearly polarized plane wave, two circularly polarized plane waves having opposite handedness are produced. One of them is forward wave while the other is backward wave which yields phenomenon of negative refraction in chiral nihility metamaterial.

If a perfect electric conductor (PEC) interface placed in chiral nihility metamaterial is excited by a forward plane wave. Only one reflected wave parallel to the incident wave is produced, i.e., negative reflection happens. The reflected wave is backward wave which cancels the incident forward wave to produce zero power propagation. Interestingly, if a chiral nihility slab backed by PEC interface is excited by linearly polarized plane wave, effect of each eigenwave in chiral nihility after reflection from PEC interface is canceled leading to a situation as if front face of the geometry is PEC and there is no chiral slab [21]. A PEC waveguide coated with chiral nihility metamaterial confines propagation of power within un-coated region of the guide [22].

In electromagnetics, Brewster angle is defined as angle of incidence for which reflection power is zero. In all introductory text books on electromagnetic theory [23,24],

reflection of vertically polarized (parallel polarized or transverse magnetic (TM)) plane wave and horizontally polarized (perpendicular polarized or transverse electric (TE)) plane wave from a dielectric-dielectric half space boundary is usually presented to explain the concept of Brewster angle. It is mentioned that vertically polarized wave experiences zero reflection at one incident angle whereas for all angles, reflection is non-zero for horizontal polarization. This means that if dielectric-dielectric half space is excited by a wave, having both the vertical and horizontal polarizations, at the Brewster angle the reflected wave will be linearly polarized with horizontal polarization only. The angle of incidence that allows total reflection of power from a planar dielectric-dielectric interface is known as critical angle. Critical angle exists only for perpendicular polarization if the wave propagates from a denser dielectric medium to a rare dielectric.

In the same context, reflection of plane wave from an interface of an achiral dielectric and a chiral/chiral nihility metamaterial was discussed by Qiu et al. [25]. Their study reveals that for certain values of constitutive parameters, the results similar and opposite to that of conventional dielectric-dielectric interface can also be achieved, that is, existence of zero reflection for only parallel polarization in the dielectric-chiral case. They also showed that, for certain values it is possible to have no-Brewster angle for both polarizations and total reflection can be achieved for a wide range of incident angles. Power corresponding to the electromagnetic waves associated with a planar interface of two chiral and/or chiral nihility metamaterials was studied by Faiz et al. [26] when it is excited by a plane wave. Using numerical results, interesting characteristics such as complete power transmission/rejection and band pass/band reject filter were observed.

1.1. GO Field and Maslov's Method

Geometrical optics (GO) is a powerful tool for the study of wave motion at high frequencies [27-29], however it fails at the caustics. A caustic is a region where the area of a ray tube is zero and hence introduces a mathematical singularity when the intensity per unit area is needed to be counted though physically this is not the case. Physically the field is always finite at caustics and caustics are of practical interest in many applications including defense and medical sciences. Maslov proposed an alternative method to find the fields in the caustic region [30]. Maslov's method combines the simplicity of asymptotic ray theory and the generality of the Fourier transform method. This is achieved by representing the GO fields in terms of mixed coordinates consisting of wave vector coordinates and space coordinates. Maslov's method is applied to study the field near the caustics of the focusing systems by many authors [31-40]. Focusing from a PEC cylindrical and spherical reflectors using Maslov's method was first treated by Hongo and Ji [33]. Faryad and Naqvi extended this work for a reflector coated with chiral metamaterial [39]. Illahi and Naqvi studied the focusing from a chiral nihility coated PEC and perfect electromagnetic conductor (PEMC) cylindrical reflector [41]. In the present work, one interest is also to unify all these cases so that these become special cases of the geometry, under investigation.

Consider the three-dimensional vector wave equation, in Cartesian coordinates $r = (x, y, z)$, describing the field in a medium having wavenumber k_0

$$\nabla^2 \mathbf{U}(r) + k_0^2 \mathbf{U}(r) = 0$$

Expressing the solution $\mathbf{U}(r)$ of the wave equation in terms of the well-known Luneberg-Kline series yields the Eikonal equation for the phase $s(r)$ and the transport equation for the amplitude. For

homogeneous and lossless medium, Eikonal equation reduces to Hamiltonian equation as

$$H(\mathbf{r}, \mathbf{p}) = (\mathbf{p} \cdot \mathbf{p} - 1)/2 = 0, \quad \mathbf{p} = \nabla s$$

where \mathbf{p} is the wave vector. The solution of Hamiltonian equation is given below

$$x = \xi + p_x t, \quad y = \eta + p_y t, \quad z = \zeta + p_z t, \quad p_x = p_{x_0}, \quad p_y = p_{y_0}, \quad p_z = p_{z_0}$$

where (ξ, η, ζ) and $(p_{x_0}, p_{y_0}, p_{z_0})$ are the initial values of cartesian coordinates (x, y, z) and wave vector coordinates (p_x, p_y, p_z) respectively and t is parameter along the ray. Finite field around caustic may be obtained using following expression obtained from Maslov's method [34,40]

$$\mathbf{U}(r) = \frac{k_0}{2\pi} \int_{-\infty}^{\infty} \int_{-\infty}^{\infty} \mathbf{E}(r_0) \left[\frac{D(t)}{D(0)} \frac{\partial(p_x, p_y)}{\partial(x, y)} \right]^{-1/2} \exp(-ik_0(s_0 + t - x(p_x, p_y, z)p_x - y(p_x, p_y, z)p_y + xp_x + yp_y)) dp_x dp_y$$

s_0 is the initial phase. Above equation provides uniform solution around the caustic region.

In this paper, transmitted and reflected powers from two parallel layers of chiral and/or chiral nihility metamaterials with respect to angle of incidence and chiralities of the layers are analyzed. Limiting cases of permittivity, with value of chirality equal to zero, are also taken into account and their interpretation are given. Focusing from a large size paraboloidal reflector, composed of two layers of chiral and/or chiral nihility metamaterials, is studied by utilizing the Maslov's method to give the remedy of GO which fails at caustic.

2.0. Formulation

Consider a geometry consisting of two infinite parallel layers of chiral metamaterials placed in air as shown in Fig. 2.1. Physical width of the two layers is taken as d_1 and d_2 , respectively. Constitutive parameters for the two layers are denoted by $(\epsilon_1, \mu_1, \kappa_1)$ and $(\epsilon_2, \mu_2, \kappa_2)$, respectively. Air in which layers are placed have constitutive parameters ϵ_0 and μ_0 .

The above mentioned geometry is excited by an oblique incident linearly polarized electromagnetic plane wave. θ_i , θ_r and θ_t are the angle of incidence, reflection and transmission with respect to the walls of layers, respectively. As chiral medium supports two circularly polarized eigen waves having different wavenumbers so fields in each layer are written as linear combination of left circularly polarized (LCP) and right circularly polarized (RCP) plane waves. Both LCP and RCP waves propagate in forward as well as backward direction in each layer. The wavenumbers of both eigen waves in a chiral media are different. Refractive indices, wavenumbers and intrinsic impedance of the medium for first chiral layer are,

$$n_{1(R,L)} = \sqrt{\epsilon_{r1}\mu_{r1}} \pm \kappa_1 \quad (7)$$

$$k_{1(R,L)} = \omega (\sqrt{\epsilon_1\mu_1} \pm \kappa_1) \quad (8)$$

$$\eta_1 = \sqrt{\frac{\mu_1}{\epsilon_1}} \quad (9)$$

where n_{1R} and k_{1R} are refractive index and wavenumber for RCP wave, respectively.

Quantity $\epsilon_{r1} = \epsilon_1/\epsilon_0$ is the relative permittivity of the medium occupying first layer.

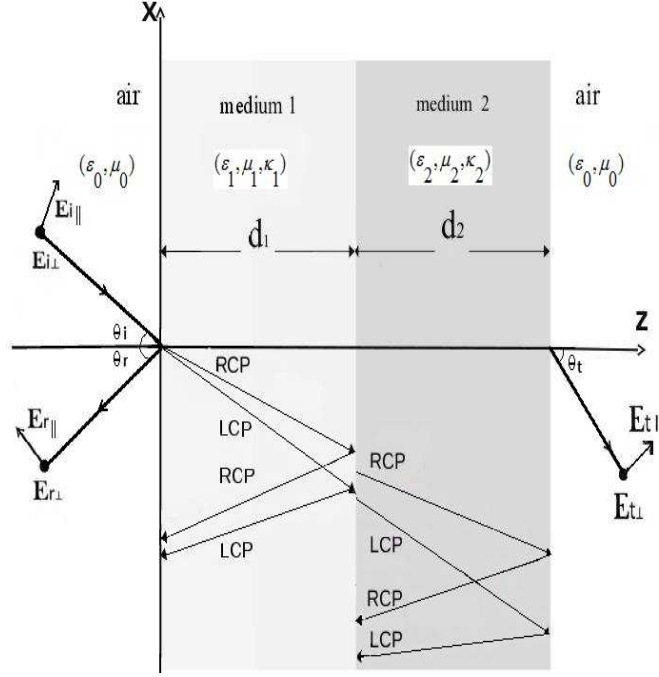


Figure 2.1. Fields representation inside and outside the layers.

For second chiral layer, these quantities are,

$$n_{2(R,L)} = \sqrt{\epsilon_{r2}\mu_{r2}} \pm \kappa_2 \quad (10)$$

$$k_{2(R,L)} = \omega (\sqrt{\epsilon_2\mu_2} \pm \kappa_2) \quad (11)$$

$$\eta_2 = \sqrt{\frac{\mu_2}{\epsilon_2}} \quad (12)$$

Wavenumber and intrinsic impedance of the host medium are given below,

$$\eta_0 = \sqrt{\mu_0/\epsilon_0} \quad (13)$$

$$k_0 = \omega \sqrt{\mu_0\epsilon_0} \quad (14)$$

Expressions for the incident and reflected fields and the field transmitted after passing through both the layers are,

$$\mathbf{E}_{\text{inc}} = [E_{i\parallel}(\mathbf{a}_z \sin \theta_i + \mathbf{a}_x \cos \theta_i) + E_{i\perp} \mathbf{a}_y] \exp[-ik_0(z \cos \theta_i - x \sin \theta_i)] \quad (15)$$

$$\mathbf{H}_{\text{inc}} = 1/\eta_0[-E_{i\perp}(\mathbf{a}_z \sin \theta_i + \mathbf{a}_x \cos \theta_i) + E_{i\parallel} \mathbf{a}_y] \exp[-ik_0(z \cos \theta_i - x \sin \theta_i)] \quad (16)$$

$$\mathbf{E}_{\text{ref}} = [E_{r\parallel}(-\mathbf{a}_z \sin \theta_r + \mathbf{a}_x \cos \theta_r) + E_{r\perp} \mathbf{a}_y] \exp[ik_0(z \cos \theta_r + x \sin \theta_r)] \quad (17)$$

$$\mathbf{H}_{\text{ref}} = 1/\eta_0[E_{r\perp}(-\mathbf{a}_z \sin \theta_r + \mathbf{a}_x \cos \theta_r) - E_{r\parallel} \mathbf{a}_y] \exp[ik_0(z \cos \theta_r + x \sin \theta_r)] \quad (18)$$

$$\mathbf{E}_{\text{tra}} = [E_{t\parallel}(\mathbf{a}_z \sin \theta_t + \mathbf{a}_x \cos \theta_t) + E_{t\perp} \mathbf{a}_y] \exp[-ik_0(z \cos \theta_t - x \sin \theta_t)] \quad (19)$$

$$\mathbf{H}_{\text{tra}} = -1/\eta_0[E_{t\perp}(\mathbf{a}_z \sin \theta_t + \mathbf{a}_x \cos \theta_t) - E_{t\parallel} \mathbf{a}_y] \exp[-ik_0(z \cos \theta_t - x \sin \theta_t)] \quad (20)$$

In above equations, $E_{r\parallel}$, $E_{r\perp}$, $E_{t\parallel}$, and $E_{t\perp}$ are unknown coefficients corresponding to parallel and perpendicular components of the respective fields.

Expressions of fields inside each chiral layer can be written as,

$$\begin{aligned} \mathbf{E}_{\mathbf{p}+} &= E_{fL}[(\mathbf{a}_x \cos \theta_{pL} + \mathbf{a}_z \sin \theta_{pL}) + i\mathbf{a}_y] \exp[-ik_{pL}(z \cos \theta_{pL} - x \sin \theta_{pL})] \\ &+ E_{fR}[(\mathbf{a}_x \cos \theta_{pR} + \mathbf{a}_z \sin \theta_{pR}) - i\mathbf{a}_y] \exp[-ik_{pR}(z \cos \theta_{pR} - x \sin \theta_{pR})] \end{aligned} \quad (21)$$

$$\begin{aligned} \mathbf{H}_{\mathbf{p}+} &= -(i/\eta_p)E_{fL}[(\mathbf{a}_x \cos \theta_{pL} + \mathbf{a}_z \sin \theta_{pL}) + i\mathbf{a}_y] \\ &\times \exp[-ik_{pL}(z \cos \theta_{pL} - x \sin \theta_{pL})] + (i/\eta_p)E_{fR}[(\mathbf{a}_x \cos \theta_{pR} + \mathbf{a}_z \sin \theta_{pR}) - i\mathbf{a}_y] \\ &\times \exp[-ik_{pR}(z \cos \theta_{pR} - x \sin \theta_{pR})] \end{aligned} \quad (22)$$

$$\begin{aligned} \mathbf{E}_{\mathbf{p}-} &= E_{bL}[(-\mathbf{a}_z \sin \theta_{pL} + \mathbf{a}_x \cos \theta_{pL}) + i\mathbf{a}_y] \exp[ik_{pL}(z \cos \theta_{pL} + x \sin \theta_{pL})] \\ &+ E_{bR}[(-\mathbf{a}_z \sin \theta_{pR} + \mathbf{a}_x \cos \theta_{pR}) - i\mathbf{a}_y] \exp[ik_{pR}(z \cos \theta_{pR} + x \sin \theta_{pR})] \end{aligned} \quad (23)$$

$$\begin{aligned} \mathbf{H}_{\mathbf{p}-} &= -(i/\eta_p)E_{bL}[(-\mathbf{a}_z \sin \theta_{pL} + \mathbf{a}_x \cos \theta_{pL}) + i\mathbf{a}_y] \\ &\times \exp[ik_{pL}(z \cos \theta_{pL} + x \sin \theta_{pL})] + (i/\eta_p)E_{bR}[(-\mathbf{a}_z \sin \theta_{pR} + \mathbf{a}_x \cos \theta_{pR}) - i\mathbf{a}_y] \\ &\times \exp[ik_{pR}(z \cos \theta_{pR} + x \sin \theta_{pR})] \end{aligned} \quad (24)$$

where k_{pL} and k_{pR} represent the wavenumbers for LCP and RCP waves, respectively.

Value of p , as 1 and 2, describes fields for first layer and the second layer, respectively.

Subscripts b and f are used to represent forward and backward waves, respectively. In above equations, E_{fL} , E_{fR} , E_{bL} , and E_{bR} are unknown coefficients. Tangential components of fields are continuous at interfaces located at $z = 0, d_1, d_1 + d_2$ and these boundary conditions are used to find the unknown coefficients. Snell's law is used to determine the relation among the angles of incidence, reflection and transmission by using following relations,

$$\theta_r = \theta_i$$

$$k_0 \sin \theta_i = k_{1(R,L)} \sin \theta_{1(R,L)} = k_{2(R,L)} \sin \theta_{2(R,L)} = k_t \sin \theta_t$$

where k_0 and k_t denote the wavenumbers for medium before and after the layers and are equal when these two layers are placed in air. Using transfer matrix method (TMM) discussed in [42], three matching matrices each relating the fields at an interface are obtained. Two 4×4 propagation matrices, linking fields between two consecutive interfaces are obtained. Numerical results for powers corresponding to parallel and perpendicular components of transmitted and reflected fields are plotted. In section 2, it is assumed that optical width of each layer is $\lambda_0/4$, where λ_0 is wave length in air corresponding to the operating frequency.

2.1. Results and Discussion

In this section, numerical results for powers corresponding to parallel and perpendicular components of the reflected and transmitted fields are presented and analyzed. Four different cases, summarized below, are considered for this purpose.

- i. Both layers are of chiral metamaterials (c-c)

- ii. First layer is of chiral nihility and second is of chiral metamaterials (cn-c)
- iii. First layer is of chiral whereas second is of chiral nihility metamaterials (c-cn)
- iv. Both layers are of chiral nihility metamaterials (cn-cn).

Results corresponding to above cases are shown by Figure 2.2 to Figure 2.9.

In addition to the above, the limiting cases of permittivity of second layer keeping $\kappa_2 = 0$ are also considered for the discussion. These cases are,

- a. First layer is of chiral metamaterial whereas permittivity of second layer is taken very large with chirality κ_2 equal to zero (c-PEC)
- b. First layer is of chiral nihility metamaterial whereas permittivity of second layer is taken very large with chirality κ_2 equal to zero (cn-PEC)
- c. First layer is of chiral metamaterial whereas permittivity of second layer is taken very small with chirality κ_2 equal to zero (c-n)
- d. First layer is of chiral nihility metamaterial whereas permittivity of second layer is taken very small with chirality κ_2 equal to zero (cn-n)

Results corresponding to above situations are shown by Figure 2.10 to Figure 2.13. \parallel and \perp signs are used to represent power for parallel and perpendicular components, respectively. For example: $c - c_{\parallel}$ and $c - c_{\perp}$ represent parallel and perpendicular components of power for chiral-chiral cases, respectively.

In Figure 2.2, powers corresponding to parallel and perpendicular components of reflected fields versus angle of incidence are shown. It is assumed that the intrinsic impedances of metamaterials filling both layers are same. Figure contains plots for four

different cases, i.e., c-c, cn-c, c-cn, and cn-cn. Brewster angle is defined as the angle of incidence for which reflection of power, both parallel and perpendicular components, is zero. Reflected powers for c-c case are zero for $\theta_i < 23^\circ$ and this gives a range of Brewster angles. In the case of cn-cn, a range of Brewster angles exists for $\theta_i < 17.5^\circ$. After this range, power for parallel component increases whereas power for perpendicular component remains negligible for the entire range of incident angles. In the case of cn-c, parallel component is nonzero everywhere and near grazing incidence almost total reflection of power happens whereas power for perpendicular component remains negligible through the entire range of incident angles. It may be noted that range of Brewster angles exist only for c-c and cn-cn cases and range of angles yielding almost total reflection exists only for parallel component of cn-c case. For c-cn case, power only for perpendicular component is zero for $\theta_i < 27.5^\circ$ and corresponding parallel component is nonzero everywhere.

Figure 2.3 describes behavior of the parallel and perpendicular components of transmitted powers for impedance matching of both layers. For c-c case, power for parallel and perpendicular components have same initial amplitude, i.e., 0.5. Considering cn-c case, power of both parallel and perpendicular components of transmitted power follow each other. In c-cn case, perpendicular component is dominant over parallel component whereas for cn-cn case, it is observed that power of parallel component is dominant over the perpendicular component.

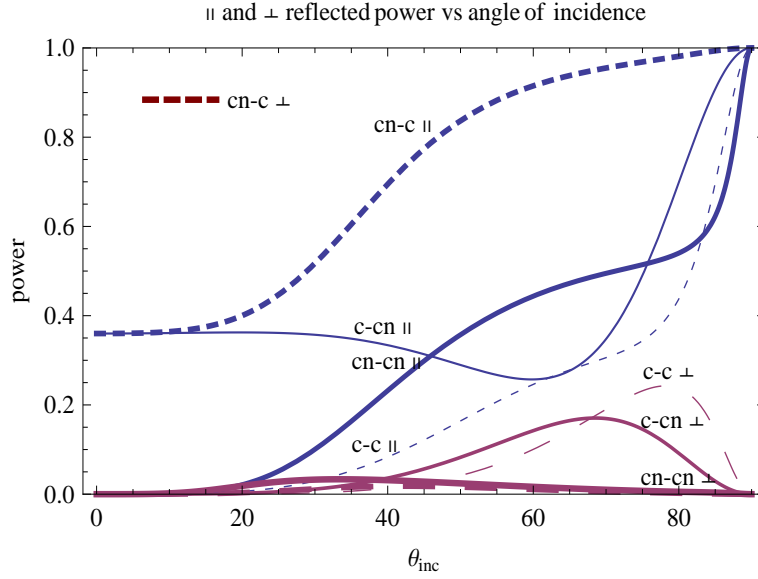


Figure 2.2. Behavior of the reflected power for parallel and perpendicular field components. $\kappa_1 = .25$, $\kappa_2 = .75$, $\eta_1 = \eta_2 = 2$

Figure 2.4 shows the behavior of reflected power for layers having different intrinsic impedances. For c-c and cn-c cases, no Brewster angle exists and power for parallel component is dominant over corresponding perpendicular component. For c-c case, reflected power only for perpendicular component is zero for $\theta_i < 34.3^\circ$ and $\theta_i > 85^\circ$. For cn-c case, when $\theta_i > 22^\circ$, power for parallel component of reflected field starts increasing and after $\theta_i = 80^\circ$, almost total reflection is observed because perpendicular component has insignificant reflected power. Perpendicular component has very low value between $\theta_i = 34.3^\circ$ and $\theta_i = 78^\circ$ and is zero elsewhere. Both c-cn and cn-cn cases have same range of Brewster angles, i.e., $\theta_i \leq 11.46^\circ$.

Figure 2.5 is about transmitted power in case of impedance mismatch. For c-c case, both components of power have equal contribution at $\theta_i = 31.5^\circ$. For cn-c and cn-cn cases, power for parallel component has higher values and follows the power for corresponding perpendicular component.

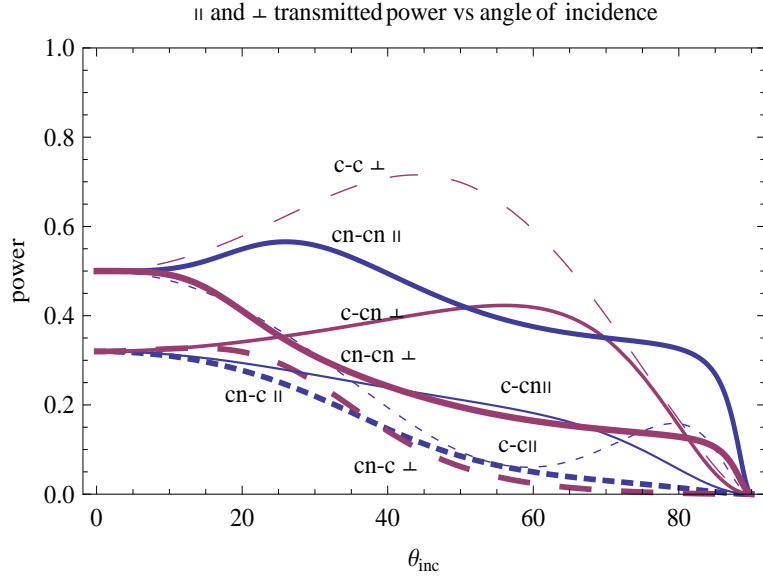


Figure 2.3. Behavior of transmitted power for parallel and perpendicular field components. $\kappa_1 = .25$ $\kappa_2 = .75$, $\eta_1 = \eta_2 = 2$

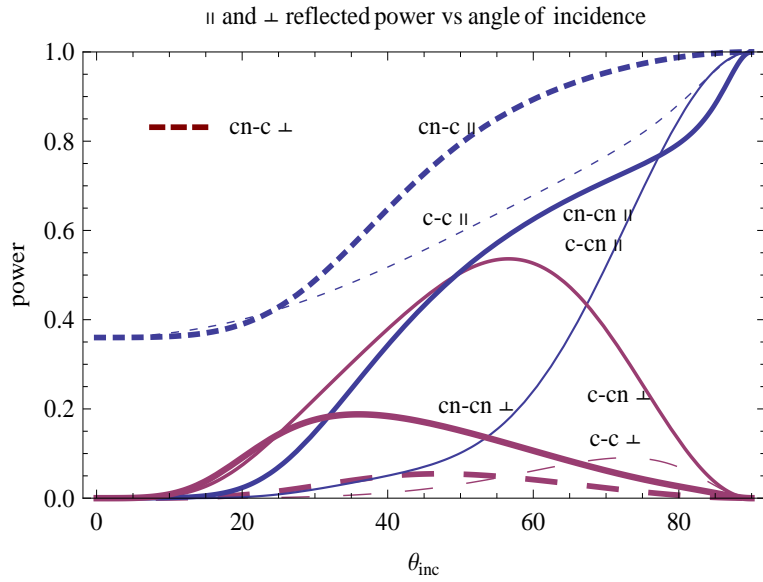


Figure 2.4. Behavior of reflected power for parallel and perpendicular field components. $\kappa_1 = \kappa_2 = .25$, $\eta_1 = 1$ and $\eta_2 = 2$

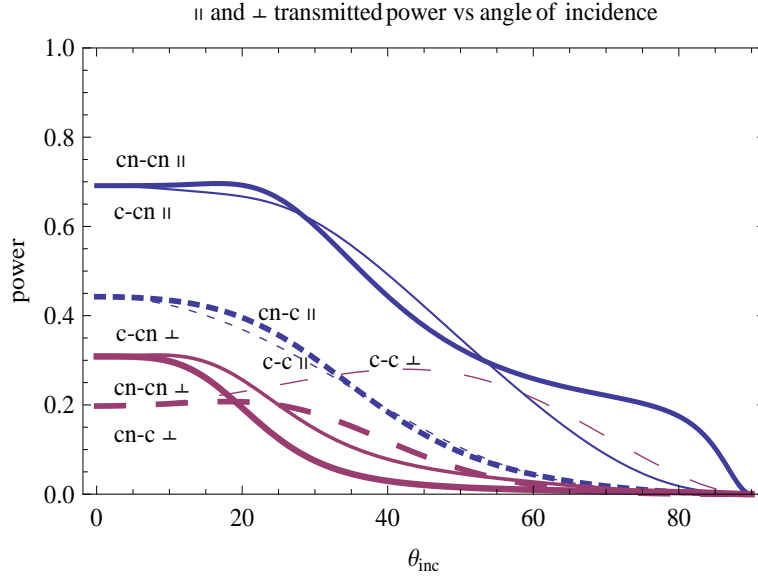


Figure 2.5. Behavior of transmitted power for parallel and perpendicular field components. $\kappa_1 = \kappa_2 = .25$, $\eta_1 = 1$ and $\eta_2 = 2$

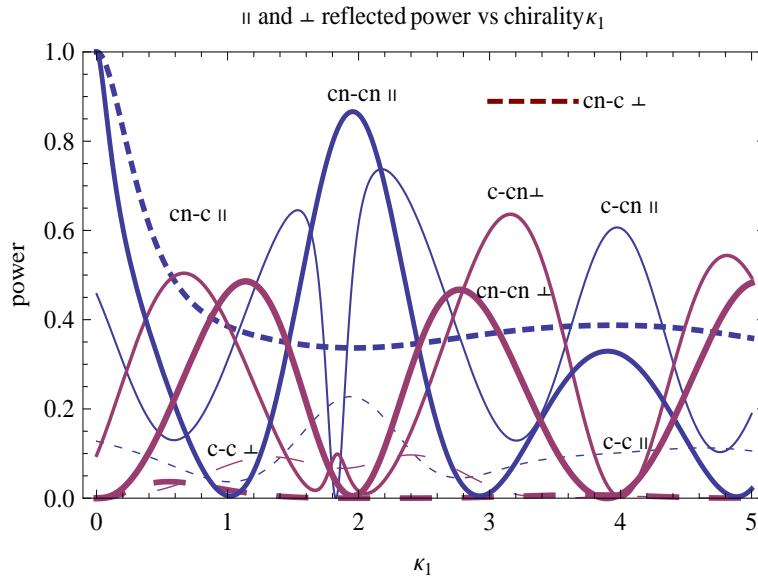


Figure 2.6. Behavior of reflected power for parallel and perpendicular field components. $\kappa_2 = .25$, $\theta_i = \pi/4$ and $\eta_1 = \eta_2 = 2$

Figure 2.6 shows plots of power for impedance matching case versus chirality of the first layer. For the purpose of analysis chirality values are considered between 0 and 5. For cn-c case, almost total power reflection in terms of parallel component occurs at very low values of chirality and perpendicular component is almost zero for considered range of chirality. For c-cn case, zero reflection of parallel power component is obtained at chirality value $\kappa_1 = 1.9$ whereas at $\kappa_1 = 1.8, 2.2, 4$ perpendicular component of reflected power is zero. In cn-cn case, oscillating behavior is observed for both components with periodic behavior for cn-cn $_{\perp}$. At $\kappa_1 = 0, 2, 4$ perpendicular component of power becomes zero and at $\kappa_1 = 1, 3, 5$ parallel component of power is zero. At $\kappa_1 = 0$, total reflection occurs. Zeros of parallel and perpendicular components of power at specific values of chirality can be used to get or avoid particular component of polarization.

Figure 2.7 gives transmission behavior of power. It is noted that both components for each case contain either zeros or values approaching to zero. These findings may be used get or avoid particular component of polarization. In Figure 2.8, no Brewster angle exist for all four cases except for cn-c case where both components are negligibly small at $k_2 = 1.9$. It is also noted that perpendicular components of power for cn-cn and cn-c are negligibly small. Conclusions similar to Figure 2.7 may be drawn from Figure 2.9.

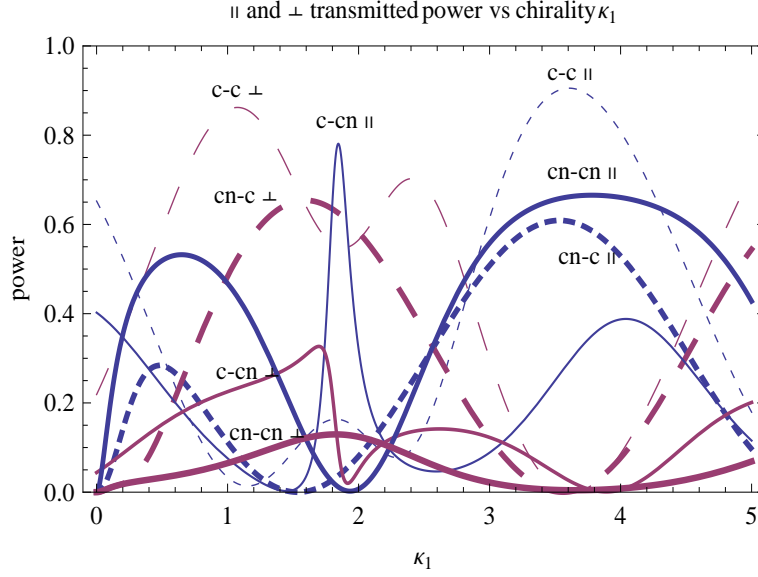


Figure 2.7. Behavior of transmitted power for parallel and perpendicular field components. $\kappa_2 = .25$, $\theta_i = \pi/4$, $\eta_1 = \eta_2 = 2$

Figure 2.10 shows the plots for reflected power assuming very high value of permittivity of second layer. This situation may be considered as a chiral layer backed by perfect electric conductor interface. In general reflected power has both components, i.e., both $c - \text{PEC}_{\parallel}$ and $c - \text{PEC}_{\perp}$ are nonzero. But for certain values of chirality of first layer, reflected field contains only co-polarized component. Contribution of parallel component is very large as compared to the perpendicular component of reflected power. For cn-PEC case, complete reflection in terms of parallel component is observed. Figure 2.11 shows zero transmission of power for $c - \text{PEC}$ and $\text{cn} - \text{PEC}$ cases.

Another interesting case is shown in Figure 2.12 where second layer is assumed of nihility metamaterial. This has been achieved by taking $\kappa_2 = 0$ and setting very low value of permittivity of second layer. This situation may be seen as a chiral layer

backed by nihility interface. For c-n case, almost total reflection in terms of parallel component of the reflected power is observed. For the case of cn-n, perpendicular component of reflected power has also significant contribution for certain range of chirality. It is noted that for certain range of chirality, overlap of cn-n and c-n cases happen. Figure 2.13 shows plots of transmitted power for c-n and cn-n cases and no transmission of power is obtained. It may be noted that conclusions drawn from Figure 2.10 to Figure 2.13 agree with published work.

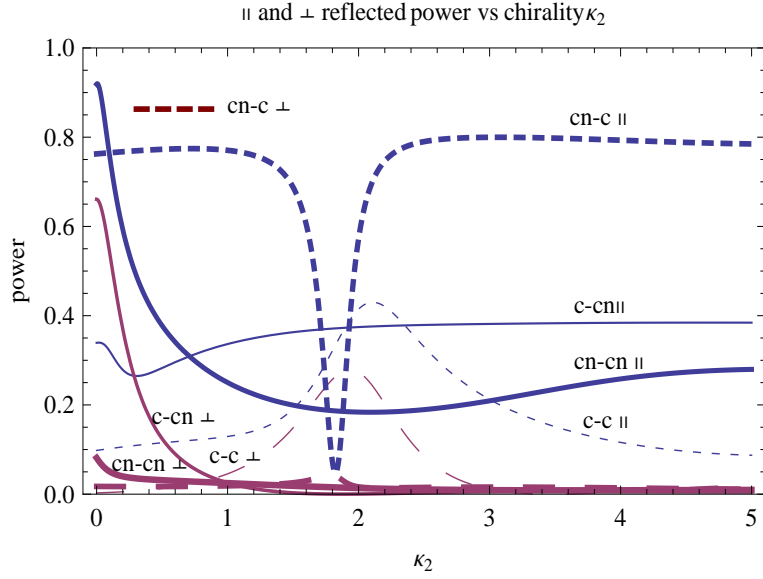


Figure 2.8. Behavior of reflected power for parallel and perpendicular field components. $\kappa_1 = .25$, $\theta_i = \pi/4$, $\eta_1 = \eta_2 = 2$

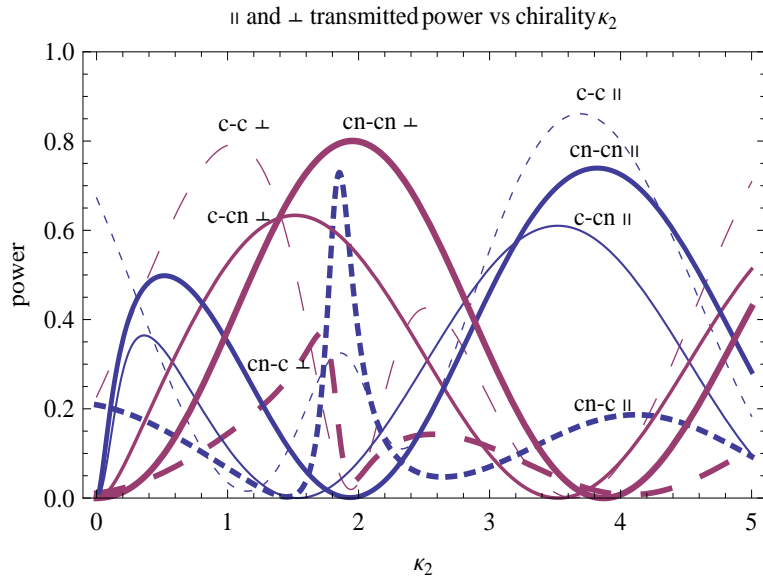


Figure 2.9. Behavior of transmitted power for parallel and perpendicular field components. $\kappa_1 = .25$, $\eta_1 = \eta_2 = 2$, and $\theta_i = \pi/4$

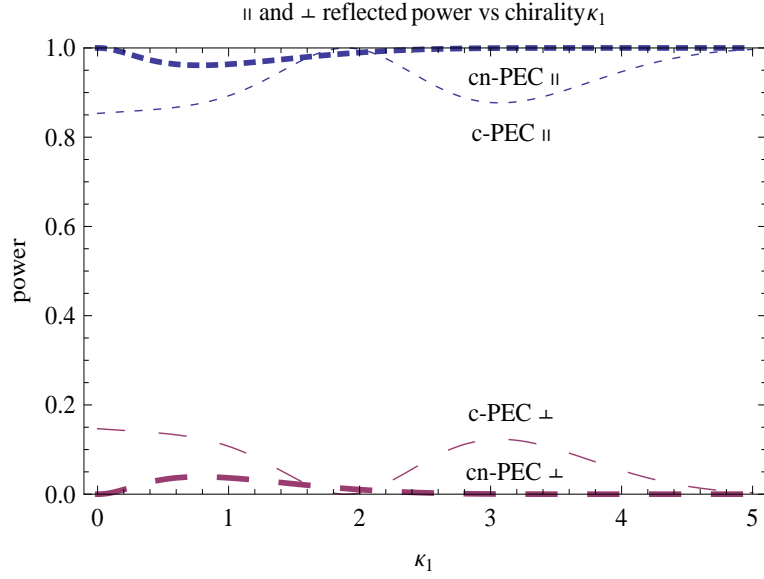


Figure 2.10. Behavior of reflected power for parallel and perpendicular field components. $\theta_i = \pi/4$, $\eta_1 = 2$, $\epsilon_2 = 10^5$, $\kappa_2 = 0$

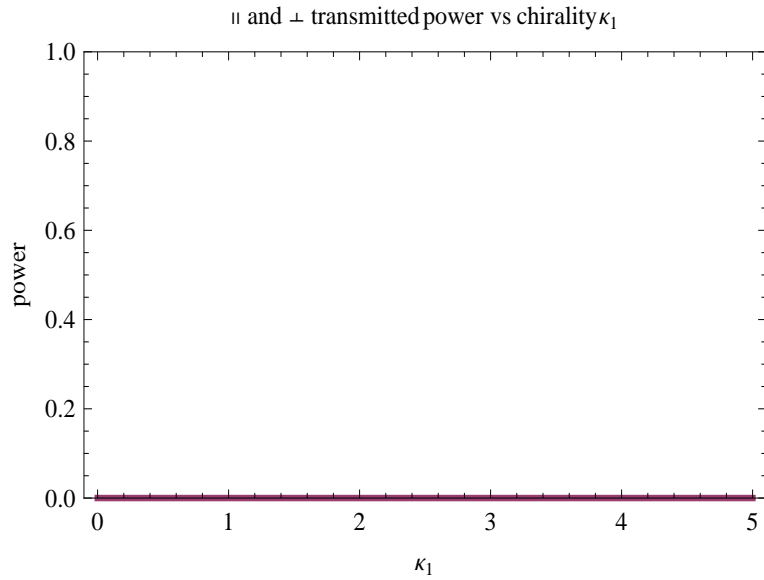


Figure 2.11. Behavior of transmitted power for parallel and perpendicular field components. $\theta_i = \pi/4$, $\eta_1 = 2$, $\epsilon_2 = 10^5$, $\kappa_2 = 0$

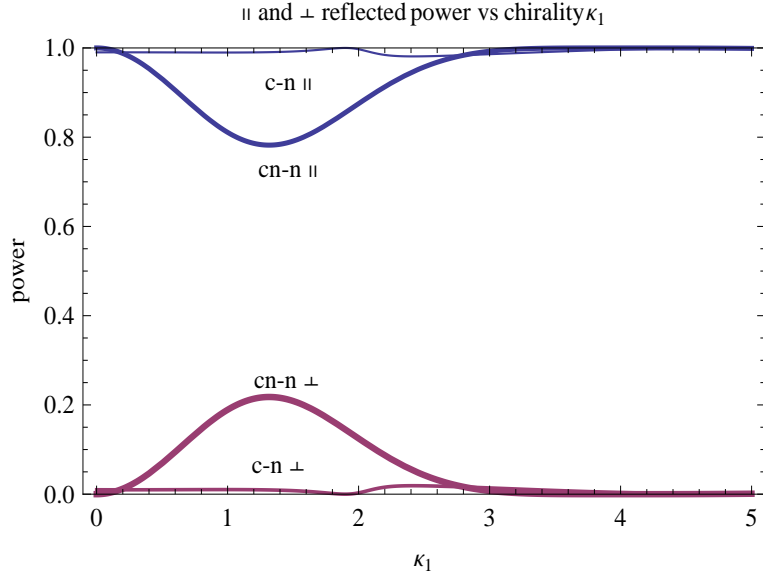


Figure 2.12. Behavior of reflected power for parallel and perpendicular field components. $\theta_i = \pi/4$, $\eta_1 = 2$, $\epsilon_2 = 10^{-5}$, $\kappa_2 = 0$

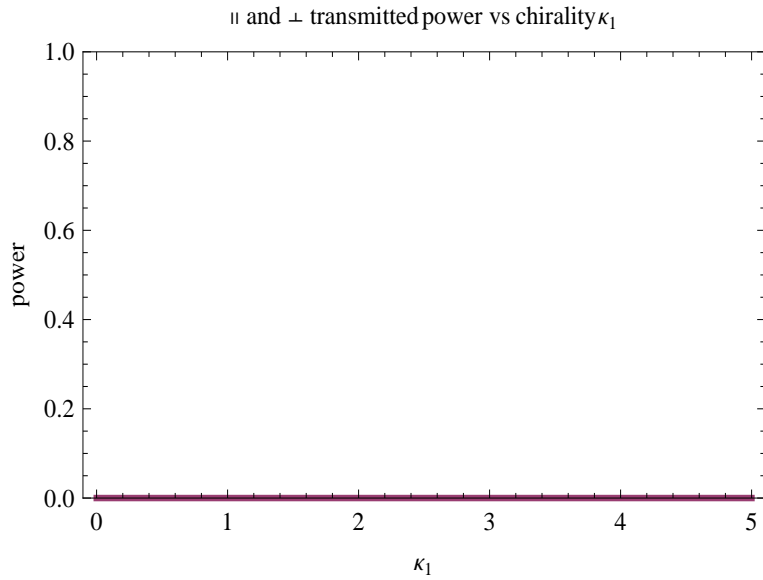


Figure 2.13. Behavior of transmitted power for parallel and perpendicular field components. $\theta_i = \pi/4$, $\eta_1 = 2$, $\epsilon_2 = 10^{-5}$, $\kappa_2 = 0$

Focusing of electromagnetic waves from a paraboloidal reflector composed of chiral and/or chiral nihility metamaterial using the Maslov's method is studied in next section. PEC and nihility backed chiral/chiral nihility paraboloidal reflector are also discussed.

3.0 Evaluation of Finite Field Around Focus

Considered a bilayer paraboloidal reflector placed in air as shown in Figure 3.0. The equation for the surface of a paraboloidal reflector is given by,

$$\zeta = f(\xi, \eta) = f - \frac{\rho^2}{4f} = f - \frac{\xi^2 + \eta^2}{4f} \quad (26)$$

where (ξ, η, ζ) are the Cartesian coordinate of the point on the surface of paraboloidal reflector. f is the focal length of the paraboloidal reflector and $\rho^2 = \xi^2 + \eta^2$.

The incident field traveling along z axis is expressed as,

$$\mathbf{E}_i = \mathbf{a}_x \exp(-ik_0z) \quad (27)$$

The incident plane wave make an angle α with surface normal, where surface normal is given as,

$$\mathbf{a}_n = \sin \alpha \cos \gamma \mathbf{a}_x + \sin \alpha \sin \gamma \mathbf{a}_y + \cos \alpha \mathbf{a}_z \quad (28)$$

where α and γ are given as,

$$\sin \alpha = \frac{\rho}{\sqrt{\rho^2 + 4f^2}}, \quad (29)$$

$$\cos \alpha = \frac{2f}{\sqrt{\rho^2 + 4f^2}}, \quad (30)$$

$$\tan \gamma = \frac{\eta}{\xi} \quad (31)$$

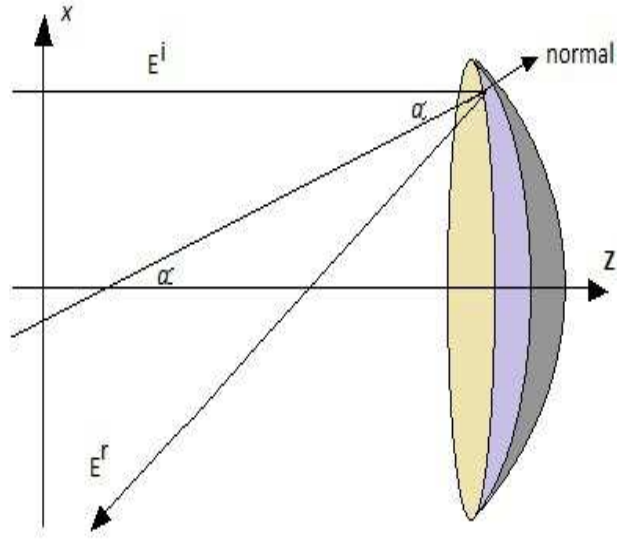


Figure 3.0. Reflection from a paraboloidal reflector placed in air

The wave reflected from paraboloidal reflector is given below,

$$\mathbf{E}_r = \mathbf{E}(r_0) \exp[ik_0(x \sin 2\alpha \cos \gamma + y \sin 2\alpha \sin \gamma + z \cos 2\alpha)] \quad (32)$$

Rectangular components of field $\mathbf{E}(r_0)$, at the surface of reflector, are given below,

$$E_{x0} = B_{\perp} \sin^2 \gamma - B_{\parallel} \cos^2 \gamma \cos 2\alpha \quad (33)$$

$$E_{y0} = -\cos \gamma \sin \gamma (B_{\parallel} \cos 2\alpha + B_{\perp}) \quad (34)$$

$$E_{z0} = B_{\parallel} \sin 2\alpha \cos \gamma \quad (35)$$

where B_{\parallel} and B_{\perp} are parallel and perpendicular components of GO reflected field from planar layers of chiral and/or chiral nihility layers. The field expression in polar coordinates and valid around the focal point is given below [40],

$$\mathbf{E}_r = \frac{i2k_0f}{\pi} \int_0^H \int_0^{2\pi} \times \mathbf{E}_{r0} \tan \alpha \exp[-ik_0(2f - r \sin \theta \sin 2\alpha \cos(\phi - \gamma) - r \cos \theta \cos 2\alpha)] d\alpha d\gamma \quad (36)$$

The upper limit of integration with respect to α is taken as,

$$H = \tan^{-1} \left(\frac{D}{2f} \right)$$

where D is the height of the paraboloidal reflector from horizontal axis.

3.1 Numerical Results and Discussion

The field behavior around the focal region of a paraboloidal reflector are obtained by solving the equation, obtained using Maslov's method. Numerical results are presented with the variation of different parameters, i.e., chirality, relative permittivity and thickness of the layer. Chiral nihility is introduced as limiting case of chiral medium where value of relative permittivity and relative permeability of the chiral medium is assumed as 10^{-5} , keeping nonzero chirality whereas for nihility material, the value of chirality parameter is taken equal to zero. In all the simulations, parameters (k_0, f, H) are taken as $(1, 100, \pi/4)$. For all cases, permeability of each chiral layer is taken as unity. All plots deal with behavior of $|\mathbf{U}(r)|$ versus kz .

3.1.1 Chiral-Chiral Paraboloidal Reflector

From Figure 3.2 and Figure 3.3, it is noted that by increasing the permittivity of each layer of the paraboloidal reflector, increases the strength of electric field around

the focus. Comparison of Figures 3.2 and 3.3, also shows that strength of field around focus is more dependent on the permittivity of second layer.

In Figure 3.4 and Figure 3.5 , effects of variation of thickness of each layer of paraboloidal reflector are presented. It is noted that increase of thickness of first or second layer also increases the strength of field around focus. It is noticed that first layer has more impact on the field strength as compared to the variation of thickness of the second layer.

Figures 3.6 and 3.7 show the effect of change of chirality parameter of each layer while keeping all the other parameters fix. It is observed that increase in chirality of each layer also strengthen the field around focal point of the paraboloidal reflector. Change in chirality of first layer produces greater change in reflected field strength around the focal point as compared to chirality variation for second layer.

For the case of c-c paraboloidal reflector, some interesting features have been studied that are permittivity, chirality and thickness of each chiral layer is directly proportional to the reflector's field strength at focal point. Moreover it has been observed that, first and second layers show different effects against the variation of a particular parameter while keeping all the other parameters fix.

3.1.2 Chiral-PEC and Chiral-Nihility Paraboloidal Reflector

In this section two special cases for paraboloidal reflector are discussed one by one: paraboloidal reflector composed of c-PEC and c-n cases. Figure 3.8 shows reflected field strength for three different values of permittivity of the first layer when second layer is considered as PEC (very large value of permittivity, i.e., 10^5). It is noted that

increase in permittivity of first layer also increases the field strength at the focal point. Figure 3.9 shows that increase in the chirality of first layer correspondingly increases the field strength at the focus. In Figures 3.10 and 3.11, second layer is considered as nihility (by assuming very small values of permittivity and permeability, i.e., 10^{-5}). From Figures 3.10 and 3.11, it is observed that by increasing the values of permittivity and chirality, the field strength around the focal point also increases correspondingly.

4.0 Conclusions

Characteristics of reflected and transmitted powers from a structure of two parallel layers filled with chiral and/or chiral-nihility metamaterials are studied. Special cases of PEC and nihility backed chiral/chiral nihility layer are also discussed. It is observed that the behavior of reflected or transmitted powers strongly depend on the angle of incidence and values of constitutive parameters describing the matamaterials. For some specific values and ranges of incident angles, total reflection of power has been observed hence structure can yield range of Brewster angles. Parallel or perpendicular component of reflected/transmitted power may be selected. That is, either co-polarized or cross polarized field is produced. Similarly for some values of chirality, total reflection/ transmission of power is also observed. This arrangement of parallel layers can also be used as a power divider.

Arrangement of two parallel layers mentioned above is utilized to study the behavior of field around the focal region of a large size paraboloidal reflector. Paraboloidal reflector, composed of c-c, c-PEC and c-n layers is discussed for this purpose. PEC and nihility backed cases give higher values of reflected field around the focus as compared to composed of chiral-chiral layers. It is concluded that increase in the relative

permittivity of each layer also increases field strength around the focus. An increase in the thickness and chirality parameter of the layer also have the same effect, i.e., increase in values of these parameters yields correspondingly higher focusing of the field. It is also noted that different parameters, mentioned above, affect the strength of the field differently. Moreover in the case of c-c paraboloidal reflector, variation of a parameter for first and second layer yields different reflected field strength when all other parameters are kept constant. In this case, change in permittivity of second layer produces more variation in the reflected field strength around the focal point as compared to the first layer, whereas for change in chirality and thickness, field strength of the reflector is more sensitive for the first layer. Hence from above discussion strength of the reflected field around the paraboloidal reflector can be controlled by studying the effect of different factors. Study of focusing field strength is of great importance in defence and other electronic systems. This study provides an investigation to design an efficient reflector coated with materials having different material properties. This whole discussion suggests to get control over the focusing of the reflected field by bringing variations in the permittivity, thickness or the chirality of the corresponding layer.

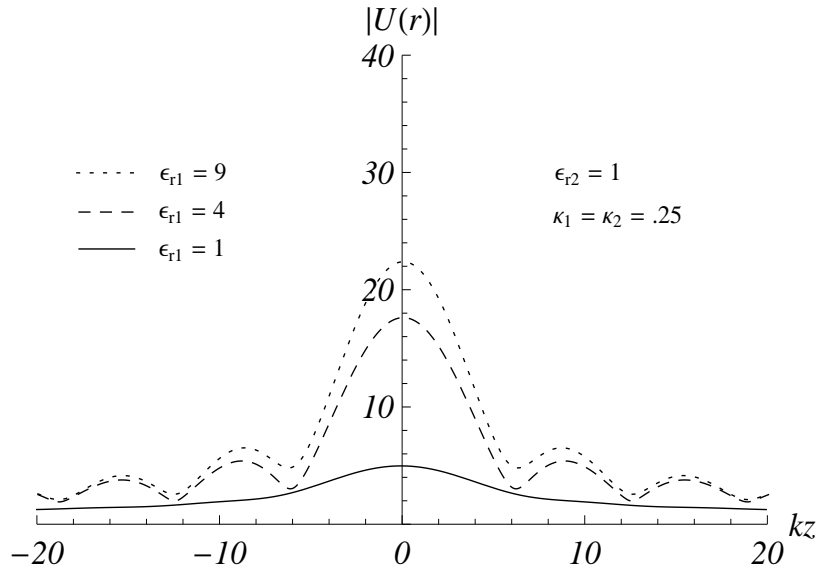


Figure 3.2. Field behavior around focus for different values of permittivity of first layer: $d_1 = d_2 = \frac{\lambda_0}{4}$, c-c case.

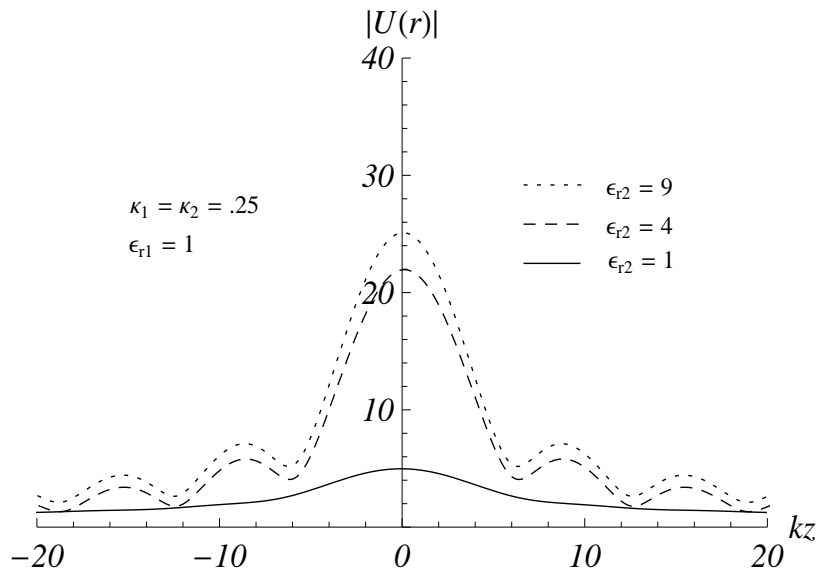


Figure 3.3. Field behavior around focus for different values of permittivity of second layer: $d_1 = d_2 = \frac{\lambda_0}{4}$, c-c case.

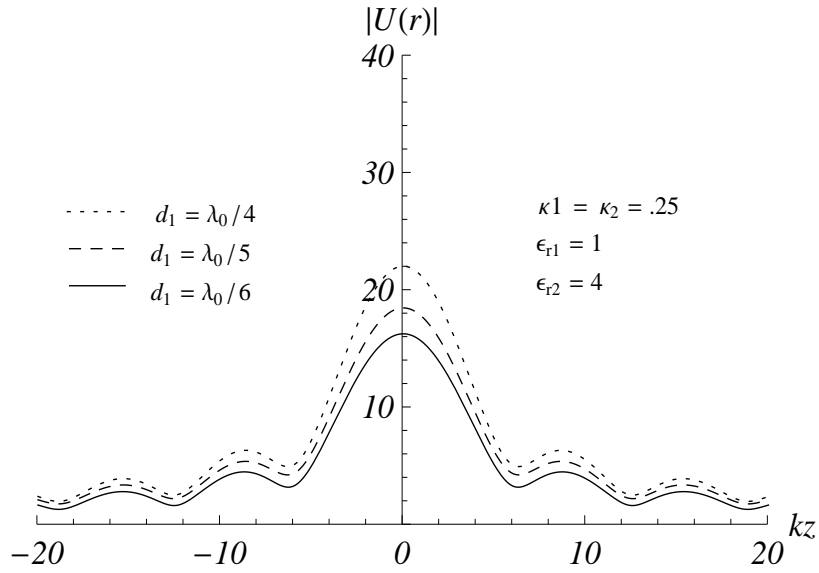


Figure 3.4. Field behavior around focus for different values of thickness of first layer: $d_2 = \frac{\lambda_0}{4}$, c-c case.

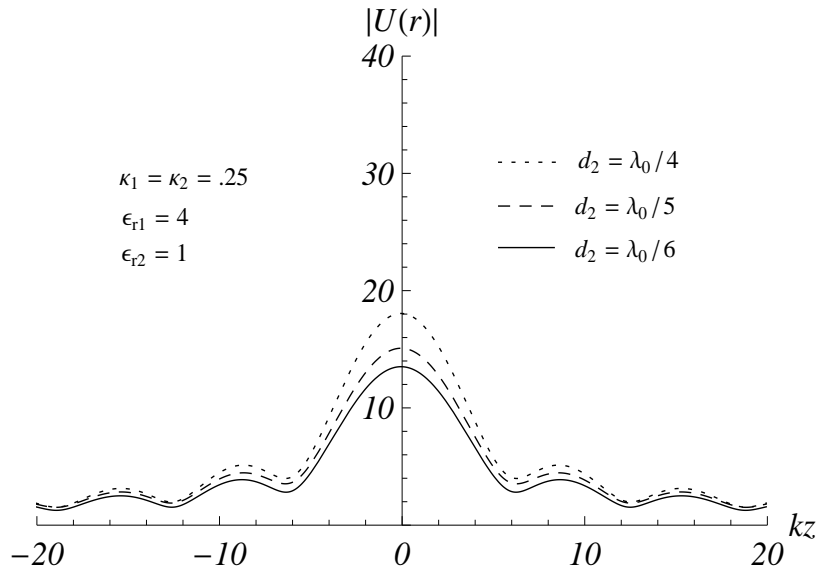


Figure 3.5. Field behavior around focus for different values of thickness of second layer: $d_1 = \frac{\lambda_0}{4}$, c-c case.

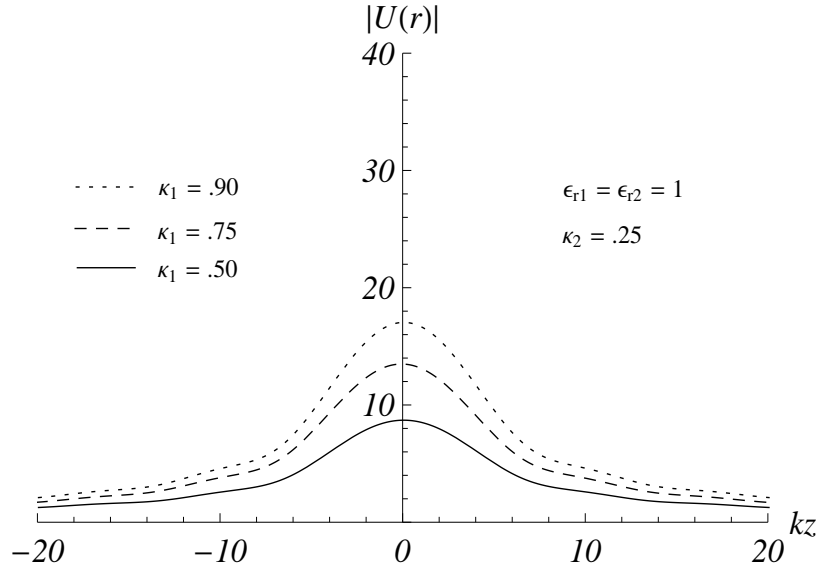


Figure 3.6. Field behavior around focus for different values of chirality of first layer:

$d_1 = d_2 = \frac{\lambda_0}{4}$, c-c case.

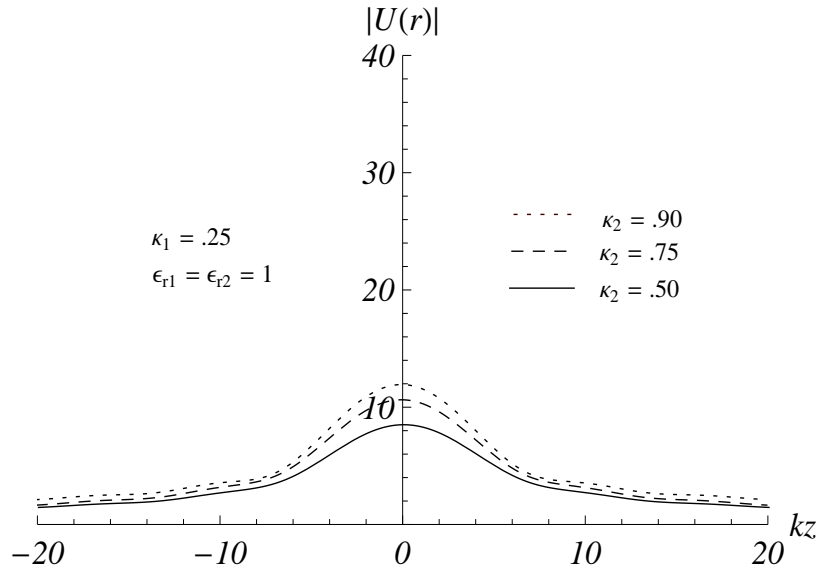


Figure 3.7. Field behavior around focus for different values of chirality parameter of

second layer: $d_1 = d_2 = \frac{\lambda_0}{4}$, c-c case.

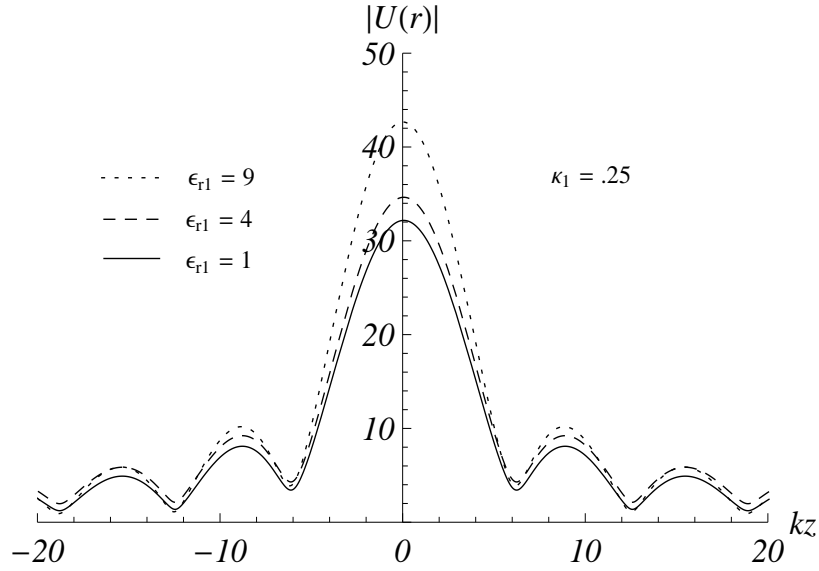


Figure 3.8. Field behavior around focus for different values of permittivity of first layer: $d_1 = d_2 = \frac{\lambda_0}{4}$, $\epsilon_{r2} = 1 \times 10^5$, c-PEC case.

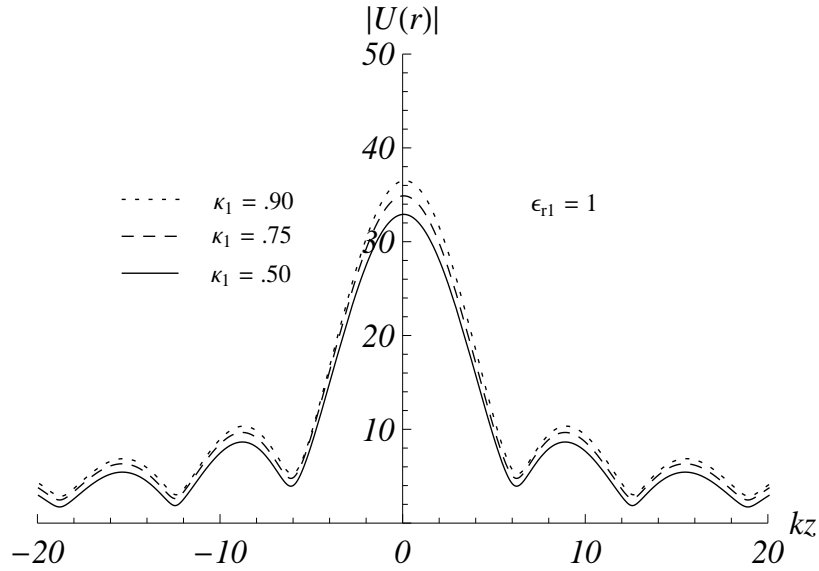


Figure 3.9. Field behavior around focus for different values of chirality of first layer: $d_1 = d_2 = \frac{\lambda_0}{4}$, $\epsilon_{r2} = 1 \times 10^5$, c-PEC case.

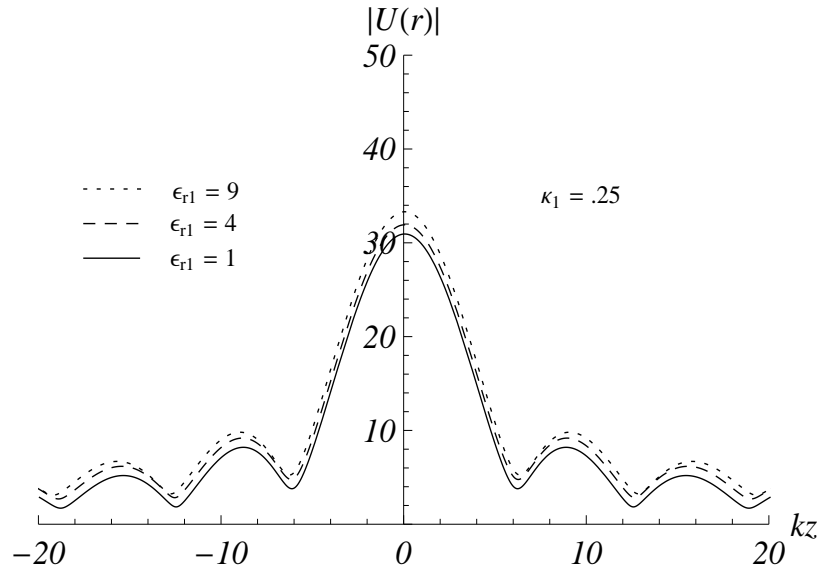


Figure 3.10. Field behavior around focus for different values of permittivity of first layer: $d_1 = \frac{\lambda_0}{4}$, $\epsilon_{r2} = 1 \times 10^{-5}$, $\kappa_2 = 0$, c-n case.

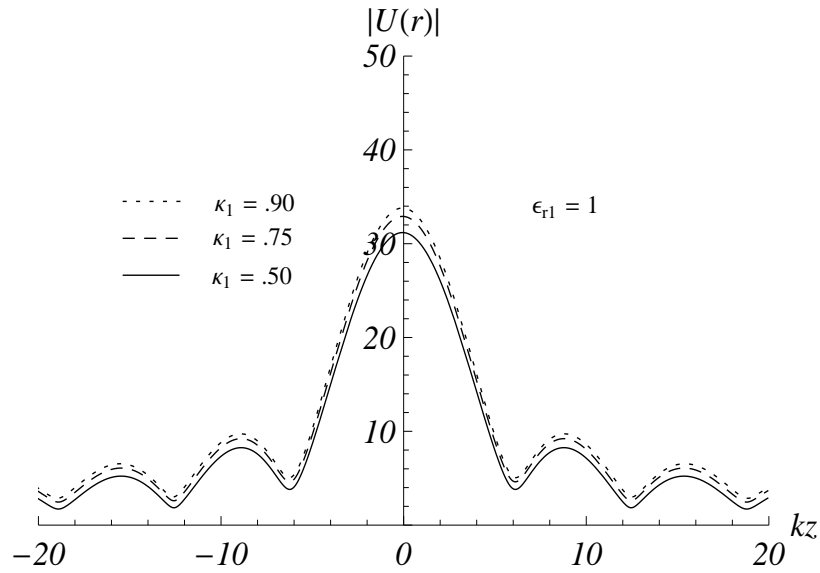


Figure 3.11. Field behavior around focus for different values of permittivity of first layer: $d_1 = \frac{\lambda_0}{4}$, $\epsilon_{r2} = 1 \times 10^{-5}$, $\kappa_2 = 0$, c-n case.

References

1. D. F. Arago, "Sur une modification remarquable qu' éprouvent les rayons lumineux dans leur passage a travers certains corps diaphanes, et sur quelques autres nouveaux phenomnes d'optique", Mem. Inst. 1, 93-134 (1811).
2. J. B. Biot, "Ph6nomenes de polarisation successive, observs dans des fluides homogenes", Bull. Soc. Philomath., 190-192 (1815).
3. A. Fresnel, "Memoire sur la double refraction que les rayons lumineux eprouvent en traversant les aiguilles de cristal de roche suivant des directions parall6les a l'axe", Oeuvres 1, 731- 751 (1822).
4. J. B. Biot, "M6moire sur la polarisation circulaire et sur ses applications a la chimie organique", Mem. Acad. Sci. 13, 39-175 (1835).
5. K. F. Lindman, "Ober eine durch ein isotropes system von spiralf6rmigen resonatoren erzeugte rotationspolarisation der elektromagnetischen wellen", Ann. Phys. 63, 621-644 (1920).
6. K. F. Lindman, "Uber die durch- ein aktives raumgitter erzeugte rotationspolarisation der elektromagnetischen wellen", Ann. Phys. 69, 270-284 (1922).
7. D. L. Jaggard, A. R. Mickelson, C. H. Papas, "On electromagnetic waves in chiral media", Appl. Phys. 18, 211-216 (1979).
8. I. V. Lindell, A. H. Sihvola, S. A. Tretyakov, A. J. Viitanen, "Electromagnetic waves in chiral and bi-isotropic media", Artech House, Boston (1994).
9. S. Bassiri, C. H. Papas, and N. Engheta , "Electromagnetic wave propagation

through a dielectric-chiral interface and through a chiral slab”, *J. Opt. Soc. of Am. A*, 5, 1450-1459 (1988).

10. A. Lakhtakia, “Beltrami fields in chiral media”, World Scientific, Singapore(1994).
11. V. G. Vaselago, “The electrodynamics of substances with simultaneously negative values of permittivity and permeability”, *Sov. Phys. Usp.* 10, 509-514 (1968).
12. C. W. Qiu, H. Y. Yao, S. Zouhdi, L. W. Li, and M. S. Leong, “On the constitutive relations of G-chiral media and the possibility to realize negative-index media”, *Microwave Opt. Technol. Lett.* 48, 2534–2538 (2006).
13. S. Tretyakov, A. Sihvola, and L. Jylh, “Backward-wave regime and negative refraction in chiral composites”, *Photonics Nanostruct. Fundam. Appl.* 3, 107–115 (2005).
14. J. B. Pendry, A. J. Holden, W. J. Stewart, and I. Youngs, “Extremely low frequency plasmons in metallic mesostructures” *Phys. Rev. Lett.* 76, 4773-4776 (1996).
15. J. B. Pendry, “A chiral route to negative refraction” *Science* 306, 1353-1355 (2004).
16. C. W. Qiu, H. Y. Yao, L. W. Li, S. Zouhdi, and T. S. Yeo, “Routes to left-handed materials by magnetoelectric couplings” *Phys. Rev. B* 75, 245214 (2007).
17. S. Zhang, Y. S. Park, J. Li, X. Lu, W. Zhang, and X. Zhang, “Negative refractive index in chiral metamaterials”, *Phys. Rev. Lett.* 102, 023901 (2009).
18. T. G. Mackay, A. Lakhtakia, Simultaneous negative- and positive-phase-velocity propagation in an isotropic chiral medium, *Microwave and Optical Technology Letters* 49, 1245-1246 (2007).

19. A. Lakhtakia, "An electromagnetic trinity from negative permittivity and negative permeability", *Int. J. Inf. and Mil. Wav.*, 22, 1731-1734 (2001)
20. S. Tretyakov, I. Nefedov, A. H. Sihvola, S. Maslovki, C. Simovski, "Waves and energy in chiral nihility", *Journal of Electromagnetic Waves and Applications* 17, 695-706 (2003).
21. Q. A. Naqvi, "Planar slab of chiral nihility metamaterial backed by fractional dual/pemc interface", *Progress In Electromagnetics Research PIER* 85, 381-391 (2008).
22. M. A. Baqir, A. A. Syed and Q. A. Naqvi, "Electromagnetic fields in a circular waveguide containing chiral nihility metamaterial" *Progress In Electromagnetics Research M* 16, 85-93 (2011).
23. C. A. Balanis, "Advanced engineering electromagnetics", John Willey and Sons, 2nd Edition (2012).
24. D. K. Cheng, "Fields and wave electromagnetics", Addison-Wesley, Newyork (1989).
25. C. W. Qiu, N. Burokur, S. Zouhdi, and L. W. Li, "Chiral nihility effects on energy flow in chiral materials", *J. Opt. Soc. of Am.*, 25, 55-63 (2008).
26. F. Ahmad, S. N. Ali, A. A. Syed, and Q. A. Naqvi, "Chiral and/or chiral nihility interfaces: parametric dependence, power tunneling and rejection" *Progress in Electromagnetics Research M* 23, 167-180 (2012).
27. L. B. Felson, *Hybrid formulation of wave Propagation and scattering*, Nato ASI Series, Martinus Nijho, Dordrecht, The Netherlands, (1984).

28. G. A. Dechamps, "Ray techniques in electromagnetics," Proc. IEEE, 60, 1022-1035 (1972).
29. C. H. Chapman and R. Drummond, "Body wave seismograms in inhomogeneous media using Maslov asymptotic theory," Bull. Seismol., Soc. Am., 72, 277-317, (1982).
30. V. P. Maslov, "Perturbation theory and asymptotic method" , Gos. Moskov., Univ., Moscow, (1965) (in Russian). (Translated into Japanese by Ouchi et al., Iwanami, Tokyo, 1976).
31. A. Ghaffar, Q. A. Naqvi, and K. Hongo, "Analysis of the fields in three dimensional Cassegrain system", Progress In Electromagnetics Research PIER 72, 215-240, (2007).
32. Y. Ji, and K. Hongo, "Analysis of electromagnetic waves refracted by a spherical dielectric interface by Maslov's method", J. Opt. Soc. Am. A, 8, 541-548 (1991).
33. Y. Ji, and K. Hongo, "Field in the focal region of a dielectric spherical by Maslov's method", J. Opt. Soc. Am. A, 8, 1721-1728 (1991).
34. K.Hongo, , Y. Ji, and E. Nakajima, "High frequency expression for the field in the caustic region of a reflector using Maslov's method", Radio Sci. 21, 911-919 (1986).
35. K. Hongo, and Y. Ji, "High frequency expression for the field in the caustic region of a cylindrical reflector using Maslov's method", Radio Sci. 22, 357-366 (1987).
36. K. Hongo, and Y. Ji, "Study of the field around the focal region of spherical reflector antenna by Maslovs method", IEEE Trans. Antennas Propagat., 36,

592-598 (1988).

37. R. W. Ziolkowski, and G. A. Deschamps, "Asymptotic evaluation of high frequency field near a caustic: an introduction to Maslov's method", *Radio Sci.* 19, 1001-1025 (1984).
38. M. Faryad, and Q. A. Naqvi, "High frequency expression for the field in the caustic region of cylindrical reflector placed in chiral medium", *Progress In Electromagnetics Research PIER* 76, 153-182 (2007).
39. M. Faryad, and Q. A. Naqvi, "High frequency expression for the field in the caustic region of a parabolic reflector coated with isotropic chiral medium," *Journal of Electromagnetic Waves and Applications* 22, 965-986 (2008).
40. T. Rahim, , M. J. Mughal, Q. A. Naqvi, and M. Faryad, "Focal region field of a paraboloidal reflector coated with isotropic chiral medium" *Progress In Electromagnetics Research PIER* 94, 351-366 (2009).
41. A. Illahi and Q. A. Naqvi "Study of focusing of electromagnetic waves reflected by a PEMC backed chiral nihility reflector using Maslov's method", *Journal of Electromagnetic Waves and Applications* 23, 863-873 (2009).
42. C. Sabah, S. Uckun "Mirrors with chiral slabs" *Journal of Optoelectronics and Advanced Materials* 8, 1918-1924 (2006).